Investigation on the Correlation Between Rheology and Morphology of PA6/ABS Blends Using Ethylene Acrylate Terpolymer as Compatibilizer

Alireza Mojarrad,[1] Yousef Jahani,[2] Mehdi Barikani[1]

[1]*Department of Polyurethane and Nanopolymers, Iran Polymer and Petrochemical Institute, Tehran, Iran*
[2]*Department of Plastics, Iran Polymer and Petrochemical Institute, Tehran, Iran*

Received 21 April 2010; accepted 9 August 2010
DOI 10.1002/app.33166
Published online 10 December 2010 in Wiley Online Library (wileyonlinelibrary.com).

ABSTRACT: Phase morphology and rheological behavior of polyamide 6 (PA6)/acrylonitrile butadiene styrene (ABS) polymers blends was studied using scanning electron microscopy and rheometry. The results showed that the phase morphology and rheological properties depends on blend composition. We evaluated the effect of addition of ABS as dispersed phase and EnBACO-MAH (ethylene *n*-butyl acrylate carbon monoxide maleic anhydride) as a compatibilizer on the morphological and rheological behaviors of PA6/ABS blends. It was concluded that there is a good agreement between the results obtained from rheological and morphological studies. As a consequence, addition of the ABS and compatibilizer weight percent led to a significant change in morphological structure and a great mounting in the viscosity as well as the elasticity. The rheological properties results demonstrate that adding compatibilizer to polymer blends led to increasing the crossover point, which shows a transition from a high viscous to a considerably more elastic behavior. Also, the slow transition of relaxation time peak from the peak of the PA6 to the peak of the ABS implies increasing the miscibility of the PA6/ABS blend components by increasing compatibilizer content. In addition, the Carreau–Yasuda model was used to extract information on rheological properties (zero shear viscosity and relaxation time) for PA6/ABS/EnBACO-MAH blends by fitting the experimental data with this model. © 2010 Wiley Periodicals, Inc. J Appl Polym Sci 120: 2173–2182, 2011

Key words: PA6/ABS blends; phase morphology; rheology behavior; Carreau–Yasuda model; relaxation time

INTRODUCTION

PA6 is a semicrystalline thermoplastic used in a wide range of engineering applications because of its attractive combination of good processability, mechanical properties, and chemical resistance to many moderately polar and nonpolar organic species.[1] However, it exhibits poor impact resistance to crack propagation in the presence of a notch, especially at low temperatures below its glass transition temperature and in the dry state, high moisture sorption, critical heat deflection temperatures, and poor dimensional stability. On the other hand, acrylonitrile butadiene styrene (ABS) polymer have been widely used in various industrial fields because of their high impact resistance, good dimensional stability, high toughness especially at lower temperatures, good processability, and good surface appearance. ABS consists of butadiene rubber dispersed in a matrix of styrene acrylonitrile copolymer. The rubber phase can improve the low-temperature toughness of PA6 and the SAN phase provides stiffness when blending ABS with PA6.[2,3] The blends of PA6 and ABS exhibit relatively poor mechanical properties due to the low interfacial tension, but their properties can be greatly improved, often with synergistic effects, through appropriate compatibilization.[4–7] A compatibilizer is often required to promote a fine dispersion, to stabilize the morphology by suppressing coalescence, and to enhance interfacial tension.[8] Therefore, the blend of PA6 with ABS has excellent properties, as evidenced by the combination of excellent toughness, outstanding chemical resistance, good dimensional stability under heat, high-quality surface finish, pleasant touch, and good moldability or ease of processing.[8,9]

The blending of miscible polymers can also lead to superior properties. A major problem can be a lack of miscibility, leading to the dispersion of large minor phase domains in the matrix of the blends. Effective compatibilization is needed to improve the interfacial adhesion between the phase components. This can be achieved by adding functionalized polymers and block or graft copolymers.[10] Melt blending of PA6 and ABS form immiscible ternary blend. These immiscible blends are thermodynamically unstable; they must be stabilized to prevent coalescence during melt blending.[11] In the development of these blends (PA6/ABS), the concept of reactive

Correspondence to: M. Barikani (m.barikani@ippi.ac.ir).

TABLE I
Detailed Compounding Formulation of PA6/ABS/Com Blends

		Constituents (wt %)		
Formulation	Compatibilized ternary blends	PA6	ABS	EnBACO-MAH
F1	PA6/ABS/EnBACO-MAH	100	0	0
F2	PA6/ABS/EnBACO-MAH	0	100	0
F3	PA6/ABS/EnBACO-MAH	75	25	0
F4	PA6/ABS/EnBACO-MAH	50	50	0
F5	PA6/ABS/EnBACO-MAH	80	15	5
F6	PA6/ABS/EnBACO-MAH	70	25	5
F7	PA6/ABS/EnBACO-MAH	60	35	5
F8	PA6/ABS/EnBACO-MAH	77.48	14.52	8
F9	PA6/ABS/EnBACO-MAH	67.78	24.22	8
F10	PA6/ABS/EnBACO-MAH	58.10	33.90	8

compatibilization and the use of styrene maleic anhydride copolymer as an efficient compatibilizer were described extensively in the past.[8,11,12] Moan et al.[13] investigated the influence of addition of a reactive compatibilizer, a random terpolymer, on morphological and rheological properties of blends of polyamide dispersed in a polyethylene matrix. This addition leads to smaller size and narrower size distribution of the dispersed phase. This has been related to the presence of copolymers at the interface, formed in situ by reaction between the PA and the terpolymer, which form an interphase between the disperse phase and the matrix. It has been demonstrated that the compatibilizer type, compatibilizer content, and blend composition on microstructure and morphology[14] all play important roles in controlling the low-temperature ductility of these blends.[15] Another method of reactive compatibilization is based on the addition of a reactive polymer to the blend as a third component. It is necessary that this reactive polymer be miscible with one of the blend components and reactive with the other blend component.[12] The addition of compatibilizer can lead to more stable and finer morphologies by reducing the effective interfacial tension.[16–19] It was expected that the co-continuous phase structure of the PA6/SAN blend would offer a good combination of the properties to the components. Many articles reported on the effects of compatibilization on morphological and rheological, of polymer blends.[13,20–25] The effects of composition and resulting morphology on rheology of blends of polyethylene and PA12, two immiscible polymers that are having the same Newtonian viscosity but different elasticity, by Huitric et al.[26] were studied. Recently, Tol et al.[27] studied the influence of rheology and reactive compatibilization on phase morphology and stability of co-continuous polyphenylene-ether/polystyrene (PPE/PS)/PA6 and PS/PA6 blends. It has been demonstrated that the uncompatibilized co-continuous morphologies are very unstable under quiescent annealing conditions and do break-up or show strong phase coarsening depending on the blend composition. Conversely, the effect of compatibilization on the phase inversion and the stability of the resulting co-continuous blend structures were investigated using scanning electron microscopy (SEM), dissolution, and extraction experiments. Also, the composition ratio of the blends (PA6 or SAN matrix) has a significant influence on the morphology and rheology of the blends, in particular for large compatibilizer concentrations.[28]

In this work, the influences of blend composition and morphology changes on the dynamic rheological behaviors of immiscible blends of PA6 and ABS compatibilized by an EnBACO-MAH copolymer were studied. Commercially, EnBACO-MAH was selected as a new compatibilizer for blending of PA6/ABS. Also, the effect of addition of ABS as dispersed phase and EnBACO-MAH as compatibilizer on the morphological and rheological behaviors of PA6/ABS blends was reported.

EXPERIMENTAL

Materials

Polyamide 6 (Ultramid B3S HP) and ABS (SD 0150) were obtained from BASF and Tabriz Petrochemical Company, respectively. A compatibilizer precursor based on EnBACO-MAH was provided by DuPont with trade name Fusabond® A MG423D with Specifications MFI (190°C, 2.16 kg): 8 g/10 min, melting point: 62°C, MAH content: 16.6 mg KOH/g.

All the materials used in this study are supplied from commercial sources. Before blending, ABS, PA6 granules were dried in oven at 80°C for 16 h, and EnBACO-MAH was dried at 80°C for 12 h. PA6/ABS/EnBACO-MAH batches at prearranged compositions were dry-mixed, and then melt blended in a twin-screw Brabender Plasticorder with a temperature profile of 235–236–237–238–239–240°C at a

screw speed of 80 rpm and feeding ratio of ~ 1 kg/h. The extrudate was water cooled and chopped into small pellets. The produced pellets were again vacuum-dried at 80°C for 16 h before injection molding. Detailed compounding formulations of PA6/ABS blends are given in Table I.

Scanning electron microscopy

A SEM of model VEGA TESCAN was used to characterize the blend morphologies. Before the SEM observations, samples were first fractured in liquid nitrogen. PA6 and ABS phases were etched by immersing the fracture surfaces in THF for 72 h at room temperature to remove the dispersed phase domains (ABS) and observe the blend phase morphologies. These samples were dried for 24 h in a vacuum oven at 80°C and gold sputtered. The microscopy operating at 20 kV was used to view the specimens, and several micrographs were taken for each sample. The size of the dispersed phase was analyzed by image analysis technique. For each blend, about 500 particles were considered to calculate these parameters. The number average diameters (D_n) and volume average diameters (D_v) were determined using the following equations.[29]

$$D_n = \frac{\sum N_i D_i}{\sum N_i} \quad (1)$$

$$D_v = \frac{\sum N_i D_i^4}{\sum N_i D_i^3} \quad (2)$$

where D_i is the diameter of each droplet and N_i is the number of droplets with a diameter of D_i.

The polydispersity (d) was also characterized by means of the ratio as shown in eq. (3):

$$d = \frac{D_v}{D_n} \quad (3)$$

Dynamic rheological measurements

A Rheometric Scientific MCR-300 controlled stress rheometer was used to measure the viscoelastic properties of the blends. Parallel plates with a diameter of 25 mm were chosen. All measurements were carried out under dry N_2 atmosphere to prevent any degradation and take-up of moisture. The following small amplitude oscillatory shear measurements were carried out for each blend at a fixed composition. Dynamic strain sweep and frequency sweep test (from 0.01 to 600 rad/s) carried out at temperature 245°C. Strain sweep tests were performed first to determine the linear viscoelastic region for each blend.

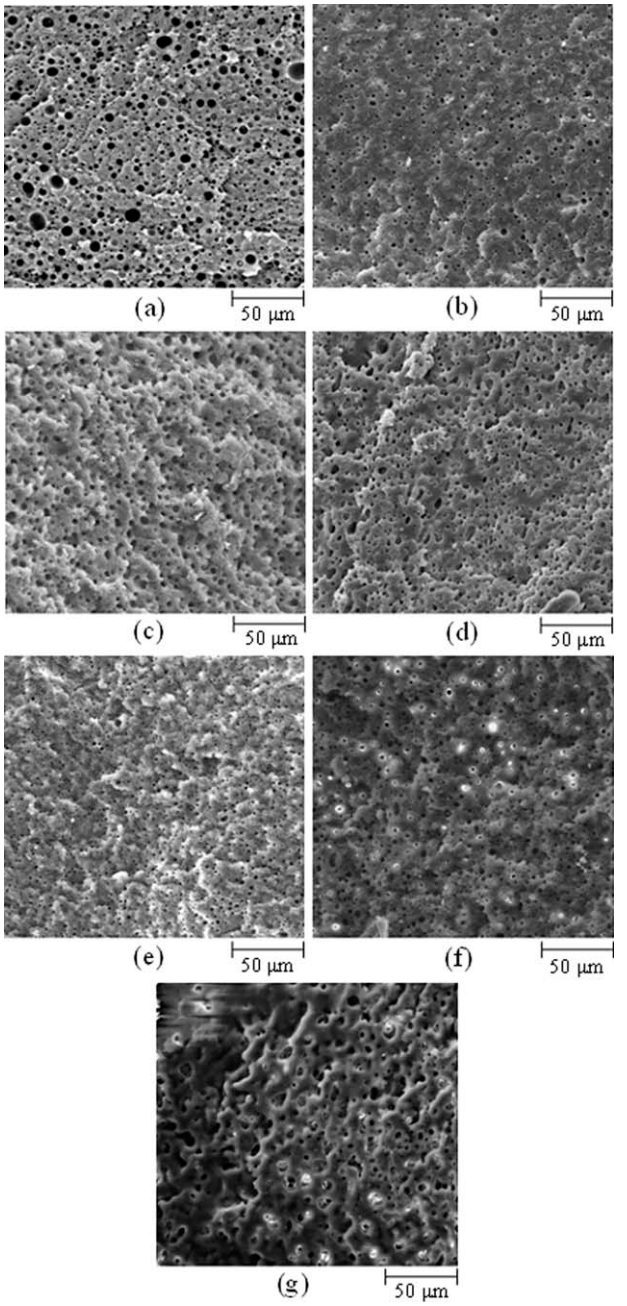

Figure 1 SEM micrographs showing the phase morphology of PA6/ABS/Com blends: (a) F3, (b) F5, (c) F6, (d) F7, (e) F8, (f) F9, and (g) F10.

RESULTS AND DISCUSSION

The effect of blend composition on morphology

Melt-blended immiscible polymer blends possess a complex phase morphology that depends on interfacial tension, volume fraction, and viscosity ratio of the components.[30] The phase morphology characteristics of blends based on various compositions of PA6/ABS/Com have been shown in Figure 1. As SEM micrographs shows the particle size diameter of ABS increases by increasing the weight percent of

ABS. To summarize, the morphology of the blends appears in a droplet matrix morphology obtained for many blends. But only for F10 blend, partial co-continuous structures is observed. On the other hand, by increasing the amount of compatibilizer the particle size diameter in dispersed phase is decreased. So in the specific content of compatibilizer (8%), the system is close to co-continuous. It can be seen that, the addition of only 35 wt % of ABS causes a significant change in blend morphology of co-continuous structure (F10). The particle size of disperse phase domains is reduced with increasing compatibilizer. Furthermore, with the addition of compatibilizer, the morphological characteristic of PA6/ABS/EnBACO-MAH blends is greatly altered. The presence of compatibilizer significantly reduces the size of the dispersed phase and shows good interfacial adhesion.[31] The effect of addition 5% compatibilizer on the morphology of PA6/ABS/Com blends is demonstrated in the SEM micrographs [Fig. 1(a–d)]. The addition of EnBACO-MAH to PA6/ABS blends led to a significant change in the morphology, we could observe that the dispersion of the minor phase was finer, and the system became more homogeneous in comparison with the samples without compatibilizer. Therefore, it is essential to determine the size of the particles and their distribution in the blends to interpret rheological data and assess rheological models.[32] When the amount of the minor phase component increases, the particles begin to coalesce and form greater structures. Further addition extends the continuous structure until the minor phase is continuous throughout the whole sample.[33] Consequently, by increasing the ABS and compatibilizer contents, the system undergoes a change from dispersed droplets–matrix structure to approximately co-continuous morphology. The volume average diameter D_v of the dispersed phase droplets as a function of the ABS concentration are shown in Table II. As shown in Table II, by increasing the weight fraction of ABS in the blend, the mean particle size increases. When the amount of ABS is 35 wt %, the mean particle size increases dramatically, which will result in extension of the particles. As the concentration of the dispersed phase increases, there is an increase in coalescence, so that the particles become progressively large and then deform into fibrils. The appearance of such a morphological structure could be associated to the blend composition, which is very close to the phase inversion composition estimated to be about 35 wt % ABS. The number average radius and volume average radius of the dispersed phase are increased by increasing of ABS content in PA6/ABS blends.

TABLE II
D_n, D_v, and d (Polydispersity) of the Dispersed Phase (ABS)

Formulation	D_n (μm)	D_v (μm)	$d = D_v/D_n$
F3	4.33213	5.57700	1.28735
F5	2.70717	3.64952	1.34809
F6	4.44776	5.10061	1.14679
F7	5.64576	9.80405	1.73653
F8	2.22950	2.39060	1.07225
F9	2.74592	3.64849	1.32869
F10	–	–	–

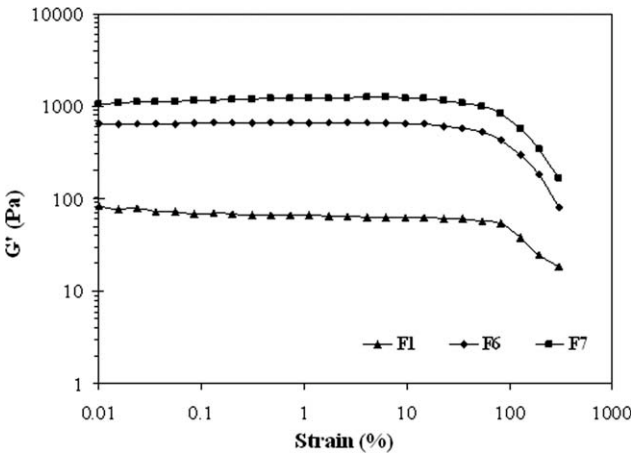

Figure 2 Storage modulus versus strain (%) for evaluation of the linear viscoelastic region at a steady frequency of 10 rad/s and 245°C.

Rheological behavior of PA6/ABS/Com blends

Dynamic strain sweep test is very much essential before performing dynamic frequency sweep test to ensure the linear viscoelastic region of the blends. That is performed at 245°C for PA6/ABS/Com blend at a steady frequency of 10 rad/s have been shown in Figure 2. These results show that the F6 and F9 blends and pure PA6 rheological behavior for strains lower than 10% at the steady frequency 10 rad/s is in linear viscoelastic region, for strains lower than 10% at the constant frequency 10 rad/s. On the other hand, the storage modulus (G') of PA6/ABS/Com blend of the ratio F9 is higher than that of two other blends, because of rising elasticity in the presence of 8% compatibilizer.

Rheological behavior of multiphase system was significantly influenced by the morphology, which depended on several parameters such as the blend composition, viscosity, and elasticity of two phases and interfacial tension.[34] The influence of compatibilizer addition and phase disperse on the variation of the complex viscosity η^* with the frequency is shown in Figure 3. According to the figure, the level of complex viscosity increases by enhancement of the concentration of added compatibilizer and ABS content. It is possibly due to an enhancement in the

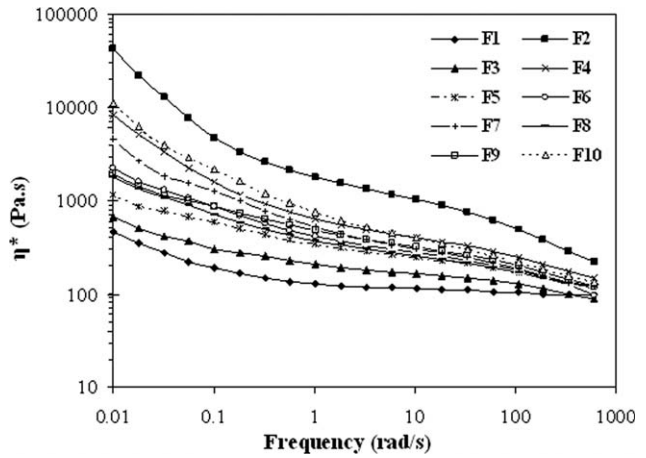

Figure 3 Complex viscosity versus frequency for the PA6/ABS/Com blends at 245°C.

interfacial interaction between the two components, which was related to the grafting reaction between MAH and the amino end groups of PA6 with the elastomeric fraction of the compatibilizer. This occurrence in F10 blend is more visible than the others. The graft copolymer formed by chemical interaction has always been dispersed in the interface between two phases, which reduces the interfacial tension and improves the compatibility.[33] When the interface is strong, the deformation of the dispersed phase would be efficiently transferred to the continuous phase; conversely, when the interface is weak, interlayer slip and disentanglement take place and hence the viscosity of the system decreases.[35] This observation suggests that at higher frequencies the incorporation of compatibilizer has not significantly affected the dynamics of the PA6 chains. But, it is clear that the compatibilizer has a considerable influence on the rheological behavior at low frequency region. It can be considered that the decreased dispersed phase is attributed to the increased viscosity by the addition of compatibilizer content.

The storage modulus G' as a function of frequency in the linear viscoelastic region for PA6/ABS/Com blends at 245°C containing different amounts of compatibilizer (5 and 8%) and ABS (15, 25, and 35%) is illustrated in Figure 4. As shown in the figure, the storage modulus represents similar trend to complex viscosity that the values of the storage modulus for all of the blends at all frequency regions increase monotonically with the addition of compatibilizer and ABS content. The storage modulus curves of all blends in all frequency regions show a similar trend, and the plateau region can be observed for some of the blends. The extended plateau region at low frequency can be related to interactions between particles. Also the evolution of the elastic modulus at low frequencies confirms the influence of the presence of physical interaction between particles. In particular, we observed that, by increasing the amount of compatibilizer, a shoulder appears in the curves of storage modulus for some of the blends. The shoulder becomes a plateau when the concentration of the compatibilizer goes beyond 5 wt %, and the plateau extends to the low frequencies region. Consequently, the increase of elasticity at low-frequency region is originated from the strong interaction between polymers and compatibilizer.[36] The presence of the compatibilizer in the blend leads to a remarkable increase in the storage modulus, which was more pronounced at low frequency.[37] The elastic modulus of the blends measured at low frequencies provides further evidence of the morphological changes. The F10 has the most elasticity among the other blends and this may be due to almost co-continuous structure. Moreover, it was interesting to note that the results obtained from morphology and rheological measurements are in good agreement.

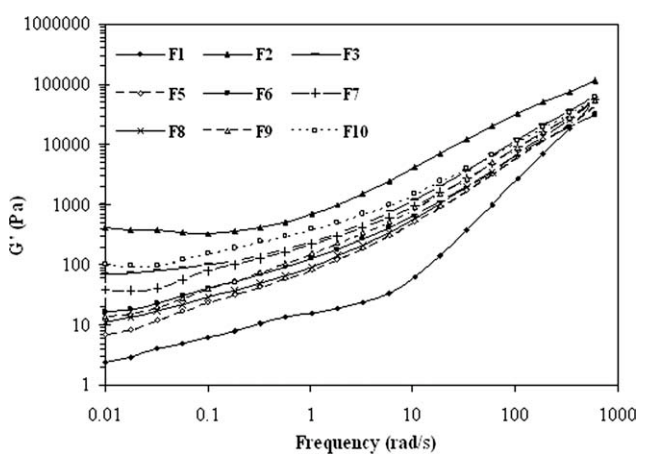

Figure 4 Storage modulus versus frequency for the PA6/ABS/Com blends at 245°C.

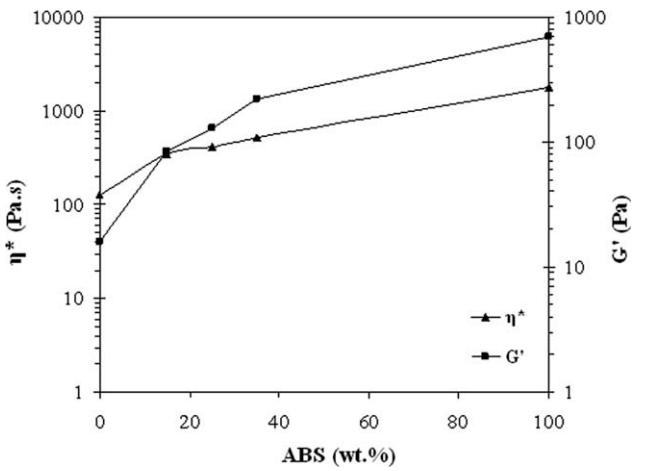

Figure 5 Storage modulus and complex viscosity versus ABS composition at frequency of 0.1 s^{-1}.

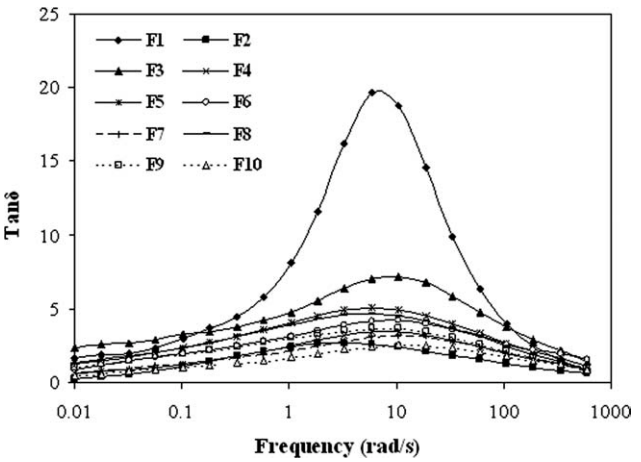

Figure 6 Damping factor versus frequency for the PA6/ABS/Com blends at 245°C.

The complex viscosity and storage modulus of all blends versus ABS composition are presented in Figure 5. According to this figure, the complex viscosity and storage modulus are increased by increasing the ABS weight fraction in all of the blends.

The plot of damping factor δ as a function of frequency is illustrated in Figure 6. According to the figure, it can be determined that PA6 has the highest damping factor at intermediate frequencies. Conversely, the F10 blend has the lowest damping factor. These results clearly indicated that for all the blends, storage modulus is raised with increasing the amount of ABS and compatibilizer, because more compatibilizer content causes higher adhesion between PA6 and ABS. Furthermore, it can be concluded that by increasing the compatibilizer content, the elastic behavior is increased followed by decreasing the damping factor.

Figure 7 clearly represents a comparison of the curves of G' versus G'' for PA6/ABS/Com blends at 245°C. It can be seen from Figure 7, at low and high frequencies region all of the blends display almost elastic, and in the intermediate frequencies region indicate viscose behavior. Moreover, this figure indicate that the addition of compatibilizer and ABS enhance the elasticity and change the morphological properties of the blends. The F10 blend has lower slope and higher elasticity than the others, as the morphological results confirm. It can be concluded that the high elasticity is related to the compatibility. Consequently, the Han plot[38] revealed that reactive compatibilization significantly increase the complex modulus of PA6/ABS blends at low frequencies.[39]

Phase inversion composition and co-continuity prediction

The resulting viscosity ratio of (PA6/ABS/Com)/ABS blends at 245°C is shown in Figure 8. As can be seen, the viscosity ratio of the high viscous ABS is higher than 10, while a value below one is observed for the blends. As shown in Figure 8, the dashed lines indicate the prediction of the phase inversion concentration in the blends with different compositions as a function of shear rate. The dashed line shows the selected content of PA6/ABS/Com in the ternary (PA6/ABS/Com)/ABS blends, the line is approximately near by the F10. At this point, the morphology changed from dispersed to almost co-continuous.[40] The morphological structure in immiscible blends is strongly related to the rheological behavior of the blend components. The concentration at which phase inversion in immiscible blends occurs can also be determined from the rheological criteria that are maximum dynamic viscosity, maximum storage modulus, and minimum slope of storage modulus.[41]

Figure 9(a–h) shows G', G'', and η^* versus frequency for all of the blends. As can be seen from this figure, many of the blends indicated two crossovers at low and high frequencies that the G' and G''

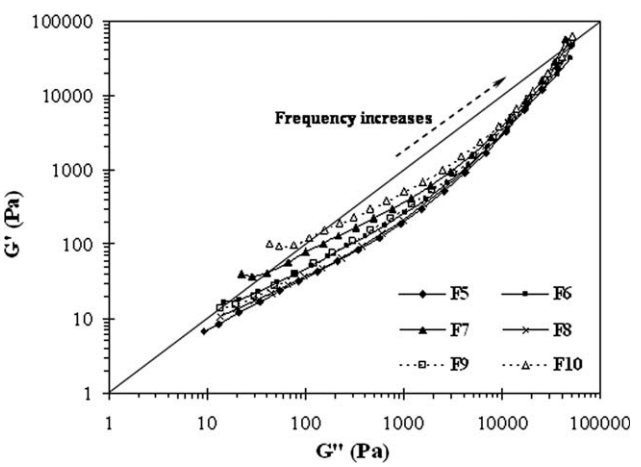

Figure 7 Han plot of the PA6/ABS/Com blends at 245°C.

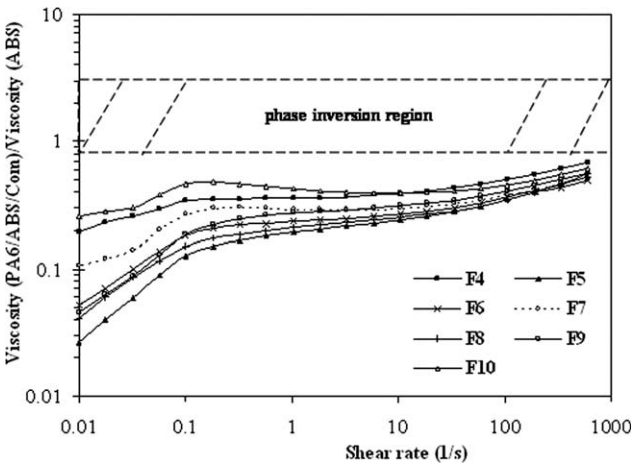

Figure 8 Viscosity ratios of the PA6/ABS/Com blends versus ABS as a function of shear rate at 245°C.

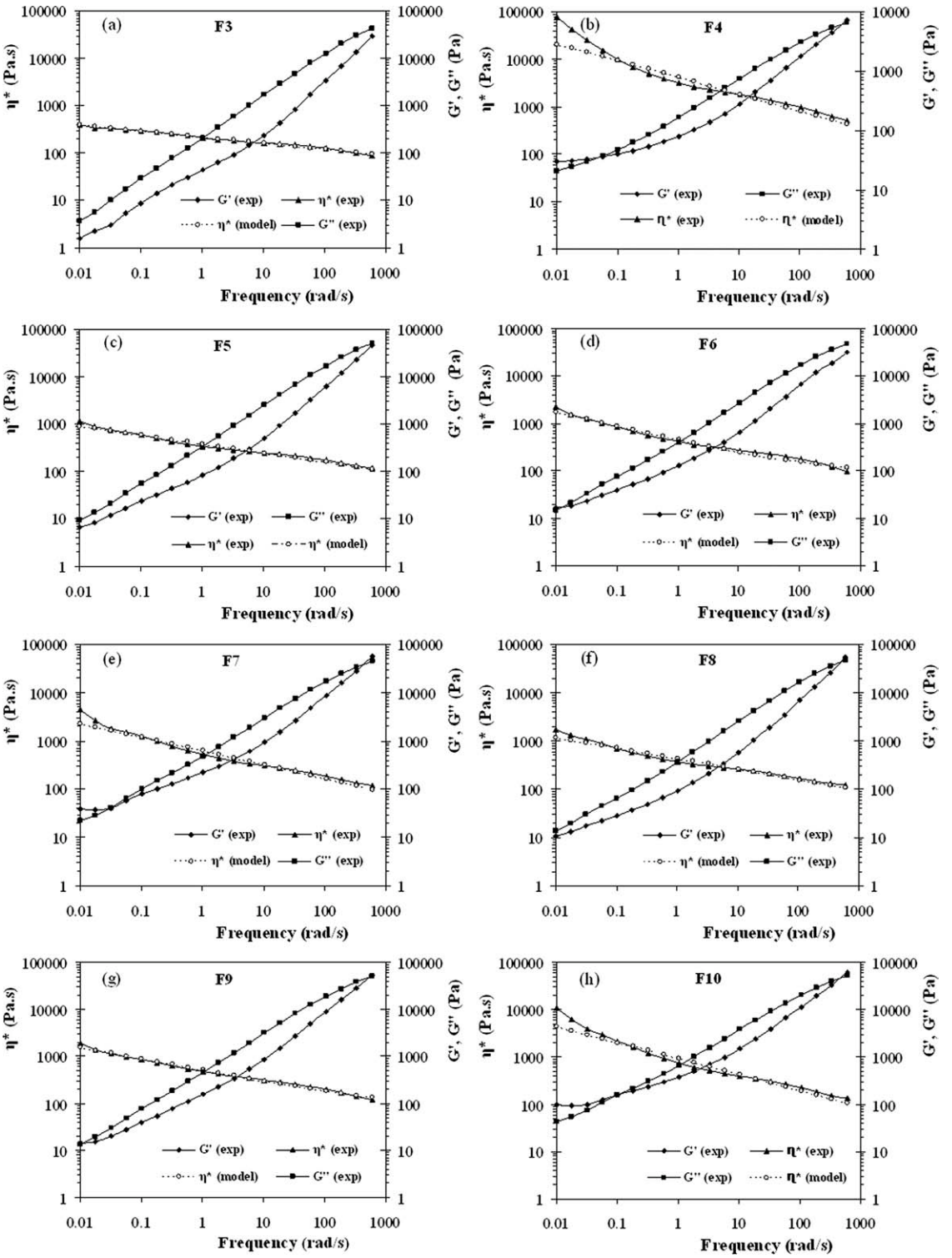

Figure 9 G', G'', and η* versus frequency and fit of the η* data to Carreau-Yasuda model for PA6/ABS/Com blends: (a) F3, (b) F4, (c) F5, (d) F6, (e) F7, (f) F8, (g) F9, and (h) F10.

crossed each other. It means that the melt behavior of blend is viscose between two crossovers. In the region of two crossing points amount of G'' is more than G'. Rheological behaviors of PA6/ABS/Com blends (F3 and F4) have been shown in Figure 9(a,b). As can be seen, by addition 25% and 50% ABS to PA6 in frequency between 0.01 to 600 rad/s the amount of G', G'', and η* have significantly increased. Figure 9(c) shows rheological behavior of a blend containing 15% ABS and 5% compatibilizer. In this figure, the values of G' and G'' are close to each other. This means that by adding 15% ABS and

TABLE III
η_0, η_∞,and G_C Obtained from Fitting Carreau–Yasuda Model to the Experimental Data for the PA6/ABS/Com Blends at 245°C

Formulation	η_0 (Pa s)	η_∞ (Pa s)	G_{C1} (Pa)	G_{C2} (Pa)
F1	2.5353	116.320	–	41,100
F2	123.55	106.21	345	50,100
F4	4425.96	102.76	88.5	58,900
F5	8.6366×10^{13}	–	–	50,700
F6	–	70.673	18.1	–
F7	–	–	41	34,500
F8	6.54×10^{15}	–	–	47,700
F9	2.1451×10^{18}	46.661	13.9	50,600
F10	–	–	156	52,200

5% compatibilizer to PA6, melt elasticity in low frequency increased because of interfacial tension between PA6 and ABS declined, so two crossover become close to each other. Also, this can indicate that in frequency close to 0.01 rad/s melt behavior of blend is elastic but by increasing frequency in the first crossover the behavior of melt will be viscose. As it can be seen from Figure 9(d), by increasing ABS content to 25%, $\acute{G}$, G'', and η^* increase and low frequency crossover (ω_{C1}) shifts to higher frequency, it means that in frequency of 0.01 rad/s the melt behavior is elastic. On the other hand, by increasing weight percent of ABS, the values of G' and G'' in different frequencies in comparison with F5 blend, is closed together, so elasticity behavior increases in lower frequency. The closeness of G' and G'' curves confirm that not only increasing interfacial adhesion of PA6 and ABS but also decreasing of interfacial tension between matrix and dispersed phases in presence of 5% compatibilizer. Figure 9(e) shows F1 blend, as it is seen in this formulation, the changes are as same as two previous formulations. So it can be concluded that in three formulations with increasing ABS content from 15 to 35%, G', G'', and η^* increase and crossover become closed together and consequently melt elasticity increases. By increasing the frequency, the crossover point indicates a transition from a more viscous deformation to a more elastic behavior. The shift in crossover frequency represents the changes in molecular mobility and relaxation time behavior.[42] In low frequency by increasing ABS and compatibilizer content G_{C1} (first crossover modulus) increases in all the graphs. G_{C1} and G_{C2} (second crossover modulus) are calculated for all the samples and shown in Table III. According to Figure 9(a–h) and Table III, by increasing of compatibilizer weight fraction from 5 to 8% elasticity is raised in low frequency, or crossover is closed together because of increasing the phase interfacial adhesion between matrix and dispersed phases. Also with increasing of compatibilizer in each formulation G', G'', and η^* raise and this phenomena is the most noticeable for F10 blend.

Comparison with model predictions

The Carreau–Yasuda model was used to extrapolate the viscosity data to its zero shear limit (zero shear viscosity) of the pure components and their blends from the dynamic measurements, assuming that the Cox–Merz rule is valid for both pure components.[24,43]

$$y = \frac{\eta_0 - \eta_{\text{inf}}}{(1 + (\lambda.x)^a)^{(1-n)}} + \eta_{\text{inf}} \tag{4}$$

$$\eta_0 - \eta_{\text{inf}} > 0 \tag{5}$$

where η_0 and η_∞ are the zero shear viscosity and infinite shear viscosity, respectively, and a, n, and λ are the width of the transition range between zero shear viscosity and power law regime, power law exponent, and relaxation time, respectively. Figure 9(a–h) show the Carreau–Yasuda model predictions for η^* compared with the experimental data for all the blends. As can be seen from this figure, η^* graphs versus frequency compared experimentally through Carreau–Yasuda model prediction. As it can be seen from all formulation, experimental curves and Carreau–Yasuda model are the same for all formulation. This means that the rheological behavior of these blends in the range of frequency from 0.01 to 600 rad/s is almost justifiable with Carreau–Yasuda model. Also the complex viscosity curves were fitted with the Carreau–Yasuda model for each blend to obtain the amount of zero shear viscosity, values are reported in Table III. According to Table III, the zero shear viscosity ratio between the dispersed phase and the matrix was found at 245°C. In each graphs, experimental data and Carreau–Yasuda model have been compared together. According to these data, all the blends fitted together in the frequency of 0.01–600 rad/s. So it can be concluded that in the range of frequency from 0.01 to 600 rad/s, melt behavior is followed to Carreau–Yasuda model. Also η_0 and η_∞ constants are obtained by fitting the Carreau–Yasuda model and are shown for all samples (Table III). The comparison between model prediction and experimental results shows the model predictions obtained for η^* and η_0 are in good agreement with the experimental data in many frequencies.

Relaxation behavior

Relaxation time spectra were provided more information about miscibility of these materials in the melt state.[44,45] A method suggested by Gramespacher and Meissner[46] consists of plotting the relaxation time spectra $H(\lambda).\lambda$ versus λ (relaxation time) and using the location of the maximum in the resulting curve as the relaxation time for the droplets.[45]

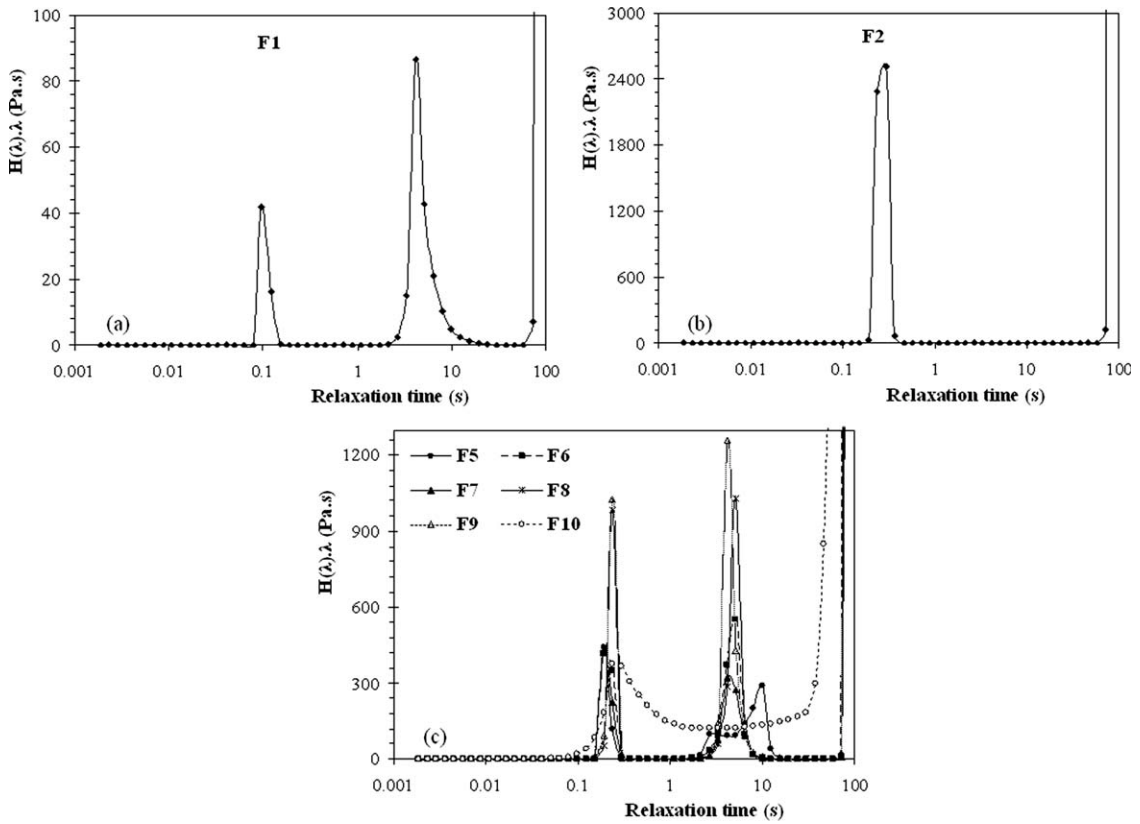

Figure 10 Relaxation time spectra of PA6/ABS/Com blends of varying ABS and compatibilizer contents at 245°C: (a) F1, (b) F2, and (c) all of the blends.

The rheological material functions G' and G'' were used to calculate relaxation time spectra and to determine characteristic relaxation times.[47] The Carreau–Yasuda model used to determine the zero shear viscosity and relaxation time.

$$\eta = (\eta_0 - \eta_\infty) \times (1 + (\lambda.x)^a)^{\frac{(n-1)}{a}} + \eta_\infty \qquad (6)$$

where η_0 and η_∞ are the zero shear viscosity and infinite shear viscosity, respectively, and λ is the relaxation time. Figure 10(a–c) shows the relaxation time spectra as a function of relaxation time for PA6/ABS/Com uncompatibilized and compatibilized blends at 245°C, calculated from the experimental storage modulus data obtained by a nonlinear spectrum calculation method,[33] available in MCR-300 rheometer software. We can see that the relaxation time spectra of the PA6 represent two peaks that is a characteristic relaxation time. Also, we observe that many blends display two peaks that are higher than that of PA6. Furthermore, all of the blends peak slightly shifted toward a higher relaxation time from that of PA6 to that of ABS. The behavior described in Figure 10(c), implies immiscibility of PA6 and ABS, and is associated with deformation of droplets of the dispersed phase. The transition from peak of the PA6 to the ABS implies increasing the miscibility of the PA6/ABS blend components by increasing compatibilizer concentration.[48] This behavior implies miscibility and compatibility of the PA6/ABS blends component. However, at high compatibilizer levels, suppresses coalescence in the all blends and, hence, properties such as relaxation time is dominated by the effects of coalescence suppression.[48] Upon more increase in the amount of compatibilizer to 8%, the slow relaxation time moves to higher. Addition of 3% compatibilizer to F7 blend raises the relaxation time. Such an increase of relaxation time with compatibilizer has been previously outstanding for F10 blend. This increase in relaxation time indicates a decrease in disperse phase droplets, although there may not be an exact proportionality between disperse phase droplets size and relaxation time in compatibilized blends.[49] When the dispersed phase content increases, the diameter of the dispersed phase droplet increases and the relaxation process of the dispersed phase becomes extended, leading to an increase of the elastic modulus.[14] This is attributed to the increase of the interfacial area as a result of diminishing the dispersed phase droplets by addition of the compatibilizer.[50]

CONCLUSIONS

In this work, the influences of blend composition and morphology changes on the dynamic rheological behaviors of immiscible blends of PA6 and ABS compatibilized by an EnBACO-MAH copolymer were studied. For this purpose, blends based on PA6/ABS with different compositions of PA6 and ABS with and without compatibilizer were investigated. It was concluded that there is a good agreement between the results obtained from rheological and morphological studies. The results clearly show the blend microstructure variations are significantly dependent on the rheological properties of the components. Conversely, the transient blend rheological behavior is closely related to the morphology changes. Rheology and morphology behavior of PA6 and ABS blends showed the effect of viscosity and elasticity ratios on the blend morphology improvement. Moreover, addition of the EnBACO-MAH and ABS leads to a significant change in morphology structure and also increased the viscosity as well as the elasticity. In addition, the Carreau–Yasuda model was used to extract information on rheological properties for PA6/ABS/Com blends, in each case the graphs of experimental data and Carreau–Yasuda model have been compared together. The slow transition of relaxation time peak from the peak of the PA6 to the peak of the ABS implies increasing the miscibility of the PA6/ABS blend components by increasing compatibilizer content.

References

1. Ozkoc, G.; Bayram, G.; Bayramli, E. J Appl Polym Sci 2007, 104, 926.
2. Kudva, R. A.; Keskkula, H.; Paul, D. R. Polymer 2000, 41, 239.
3. Yongjin, L.; Hiroshi, S. Macromol Rapid Commun 2005, 26, 710.
4. Majumdar, B.; Keskkula, H.; Paul, D. R. Polymer 1994, 35, 5468.
5. Majumdar, B.; Keskkula, H.; Paul, D. R. Polymer 1994, 35, 5453.
6. Majumdar, B.; Keskkula, H.; Paul, D. R. Polymer 1994, 35, 3164.
7. Lai, S. M.; Liao, Y. C.; Chen, T. W. Polym Eng Sci 2005, 45, 1461.
8. Triacca, V. J.; Ziaee, S.; Barlow, J. W.; Keskkula, H.; Paul, D. R. Polymer 1991, 32, 1401.
9. Aoki, Y.; Watanabe, M. Polym Eng Sci 1992, 32, 878.
10. Helfand, E.; Tagami, Y. J. Chem Phys 1972, 56, 3592.
11. Sundararaj, U.; Macosko, C. W. Macromolecules 1995, 28, 2647.
12. Lavengood, R. E.; Padwa, R. A.; Harris, A. F. U.S. Pat. 4,713,415 (1987).
13. Moan, M.; Huitric, J.; Médéric, P. J Rheol 2000, 44, 1227.
14. Calvaő, P. S.; Yee, M.; Demarquette, N. R. Polymer 2005, 46, 2610.
15. Kudva, R. A.; Keskkula, H.; Paul, D. R. Polymer 1998, 39, 2447.
16. Anastasiadis, S. H.; Gancarz, I.; Koberstein, J. T. Macromolecules 1989, 22, 1449.
17. Hu, W.; Koberstein, J. T.; Lingelser, J. P.; Gallot, Y. Macromolecules 1995, 28, 5209.
18. Verdier, C.; Vinagre, H. T. M.; Piau, M.; Joseph, D. D. Polymer 2000, 41, 6683.
19. Retsos, H.; Margiolaki, I.; Messaritaki, A.; Anastasiadis, S. H. Macromolecules 2001, 34, 5295.
20. Jansseune, T.; Moldenaers, P.; Mewis, J. J Rheol 2003, 47, 829.
21. van Hemelrijck, E.; van Puyvelde, P.; Macosko, C. W.; Moldenaers, P. J Rheol 2005, 49, 783.
22. Bousmina, M.; Muller, R. Rheol Acta 1996, 35, 369.
23. Germain, Y.; Ernst, B.; Genelot, O.; Dhamani, L. J Rheol 1994, 38, 681.
24. Lacroix, C.; Grmela, M.; Carreau, P. J. J Rheol 1998, 42, 41.
25. Vinckier, I.; Moldenears, P.; Mewis, J. J Rheol 1996, 40, 613.
26. Huitric, J.; Médéric, P.; Moan, M.; Jarrin, J. Polymer 1998, 39, 4849.
27. Tol, R. T.; Groeninckx, G.; Vinckier, I.; Moldenaers, P.; Mewis, J. Polymer 2004, 45, 2587.
28. Sailer, C.; Weber, M.; Steininger, H.; Handge, U. A. Rheol Acta 2009, 48, 579.
29. Zhu, L.; Xu, X.; Ye, N.; Sheng, J. Polym Compos 2010, 31, 105.
30. Oommen, Z.; Zachariah, S. R.; Thomas, S.; Groeninckx, G.; Moldenaers, P.; Mewis, J. J Appl Polym Sci 2004, 92, 252.
31. Shi, D.; Hu, G. H.; Ke, Z.; Li, R. K. Y.; Yin, J. Polymer 2006, 47, 4659.
32. Castro, M.; Prochazka, F.; Carrot, C. J Rheol 2005, 49, 149.
33. Biju, J.; Varughese, K. T.; Zachariah, O.; Sabu, T. Polym Eng Sci 2010, 50, 665.
34. Jeon, H. S.; Nakatani, A. I.; Han, C. C.; Colby, R. H. Macromolecules 2000, 33, 9732.
35. Wanjie, W.; Yanxia, C.; Jingwu, W.; Qiang, Z. J Appl Polym Sci 2009, 112, 953.
36. Kim, H. B.; Choi, J. S.; Lee, C. H.; Lim, S. T.; Jhon, M. S.; Choi, H. J. Eur Polym J 2005, 41, 679.
37. Krache, R.; Benachour, D.; Pötschke, P. J Appl Polym Sci 2004, 94, 1976.
38. Han, C. D.; Yang, H. H. J Appl Polym Sci 1987, 33, 1199.
39. Sailer, C.; Handge, U. A. Macromol Symp 2007, 254, 217.
40. Göldel, A.; Ruckdäschel, H.; Müller, A. H. E.; Pötschke, P.; Altstädt, V. E-Polymers 2008, 151, 1.
41. Steinman, S.; Gronski, W.; Friedrich, C. Rheol Acta 2002, 41, 77.
42. Jahani, Y. J Vinyl Addit Technol 2010, 16, 70.
43. Mighri, F.; Huneault, M. A.; Ajji, A.; Ko, G. H.; Watanabe, F. J Appl Polym Sci 2001, 82, 2113.
44. Fang, Y.; Carreau, P. J.; Lafleur, P. G. Polym Eng Sci 2005, 45, 1254.
45. Lacroix, C.; Aressy, M.; Carreau, P. J. Rheol Acta 1997, 36, 416.
46. Gramespacher, H.; Meissner, J. J Rheol 1992, 36, 1127.
47. Riemann, R. E.; Cantow, H. J.; Friedrich, C. Polym Bull 1996, 36, 637.
48. Mc Callum, T. J.; Kontopoulou, M.; Park, C. B.; Muliawan, E. B.; Hatzikiriakos, S. G. Polym Eng Sci 2007, 47, 1133.
49. Martin, J.; Velankar, S. J Rheol 2007, 51, 669.
50. Jafari, S. H.; Yavari, A.; Asadinezhad, A.; Khonakdar, H. A.; Böhme, F. Polymer 2005, 46, 5082.